PHILOSOPHICAL TRANSACTIONS OF THE ROYAL SOCIETY A MATHEMATICAL, PHYSICAL & ENGINEERING SCIENCES

Thermal and Petrological Consequences of Melt Migration within Mantle Plumes

Georges Ceuleneer, Marc Monnereau, Michel Rabinowicz and Christine Rosemberg

Phil. Trans. R. Soc. Lond. A 1993 **342**, 53-64
doi: 10.1098/rsta.1993.0004

Thermal and petrological consequences of melt migration within mantle plumes

By Georges Ceuleneer, Marc Monnereau, Michel Rabinowicz and Christine Rosemberg

Groupe de Recherche de Géodésie Spatiale, Centre National de la Recherche Scientifique UPR 234, 14, av. Ed. Belin, 31400 Toulouse, France

The high temperatures and high degrees of melting expected in the core of mantle plumes have virtually no expression in the eruption temperatures of hotspot lavas, nor in the composition of their glasses, which is restricted in the basaltic field. A solution to this paradox is looked for in the melt migration processes within the melting region of mantle plumes. Three dimensional convective calculations at Rayleigh number of 10^6 allow estimates of the possible temperature, melt fraction and stress fields within a plume. Two regions with different melt migration patterns can be distinguished. A lower zone ranging in depth from the base of the melting region (150 km) to around 80–100 km where the first melt fraction is redistributed in a sub-horizontal vein network and convects in response to the steep horizontal temperature gradient. This process is able to homogenize the temperature within the melting region very efficiently. The high (300 °C) temperature contrast between the centre of the plume and the surrounding mantle can be reduced to a few tens of degrees at the top of this zone. Fractional crystallization of high pressure phases will strongly modify the composition of the melt as it circulates toward the periphery of the melting region. A second upper zone, where the sub-vertical vein orientation will make possible rapid melt migration toward the surface, extends to the base of the lithosphere. Due to the buffering of the plume temperature around a value close to the mean upper mantle temperature, the degree of adiabatic melting within this upper zone will not greatly exceed that beneath normal spreading centres, even in the case of on-ridge hotspots. The lavas erupted at hotspots are likely to result from the mixing in various proportions of these low pressure melts (basalts) with the highly evolved liquids (possibly with kimberlitic to alkalic affinities) resulting from fractional crystallization of the high-pressure melt fractions produced at the base of the melting region. This scenario could account for the low eruption temperatures and Mg contents of hotspot lavas, in spite of a complex high pressure, and thus high temperature, history evidenced by some geochemical trends.

1. Introduction

A challenge for the coming years is to establish accurate relationships between the solid-state mantle convection and the chemistry of the melts erupted at the Earth surface which, for a given mantle composition, is related to parameters like the degree of melting, the depth of melt segregation and the amount of fractional crystallization (Albarède 1992; Langmuir *et al.* 1992). In that spirit, McKenzie & Bickle (1988) suggest that the mid-ocean ridge volcanism provides a largely random

Phil. Trans. R. Soc. Lond. A (1993) **342**, 53–64
Printed in Great Britain

sampling of the upper mantle far from any deep-seated upwelling and allows to estimate a mean mantle potential temperature. Their estimation (1280 °C) falls within the range of values deduced from a worldwide survey of mid-ocean ridge basalts chemistry (Klein & Langmuir 1987). Hotspots constitute another geodynamic setting where mantle partial melts are produced in abundance. Geophysical and isotopic data are largely consistent with a 'plume' origin for hotspot volcanism. Compared to environments of passive upwelling like the oceanic ridges, a complex thermal structure is expected in the mantle underlying hotspot volcanoes. Since Morgan's hypothesis relating hotspots to ascending convective currents, our understanding of hotspot dynamics has been largely conditioned by progress in the modelling of mantle convection. Thanks to the recent increase of computer power, it is now possible to perform high resolution three-dimensional (3D) convective calculations and to account for some geophysical observations related to hotspots (Rabinowicz *et al.* (1990) and references therein), and thus to check in what extent the thermal fields predicted by such convective models are consistent with the petrological composition of hotspot lavas. A characteristic shared by most models of mantle plumes is an important temperature contrast – a few hundred degrees, at least – between the core of the plumes and an average mantle geotherm, which is consistent with the occurrence of partial melts below thick lithospheric lids (White & McKenzie 1989). Surprisingly, these very high temperatures have no expression in the measured eruption temperatures of hotspot lavas: maximum values of 1190 and 1270 °C are reported for the 'picritic' (i.e. highly olivine phyric) flows of Hawaii and Iceland respectively (Jakobsson *et al.* 1978; Helz 1987). These should be compared to the eruption temperatures calculated for primitive mid-ocean ridge basalts (1140–1210 °C; Allan *et al.* 1987). The temperatures of more common hotspot tholeiitic flows overlap the field of MORB's eruption temperatures. In the present paper, we propose a possible solution to this paradox. Based on recent high-pressure melting experiments and on a 3D numerical model of convection constrained by geophysical data, we estimate the nature of melts which should be produced within a mantle plume. To account for some basic petrological characteristics of hotspot lavas, we discuss possible thermal effects of melt migration within the plume.

2. Plume model

Previous attempts to account for a 'plume' convective pattern within the mantle have shown the importance of rheological stratification. A low viscosity zone (LVZ) ranging in depth from the base of the lithosphere to about 150–200 km is required by many geophysical observations and is likely to be related to the softening of mantle peridotites as they approach, and eventually cross, their solidus. Beneath hotspot swells, a viscosity contrast of about 50 between the LVZ and the underlying mantle has been inferred from geoid and bathymetric data (Robinson *et al.* 1987; Ceuleneer *et al.* 1988). Three-dimensional calculations of convection in large rectangular boxes have shown that such a LVZ induces the formation of a hexagonal convective planform where ascending flows have the form of steady narrow plumes (Rabinowicz *et al.* 1990). This pattern results mainly from the asymmetry induced by the low viscosity zone between the upper and lower convective boundary layers. It satisfies some of the observed (or expected) properties of hotspot plumes: the extreme narrowness of the upwelling currents (of the order of several tens of kilometres at the base of the lithosphere), their location at the centre of more diffuse downwelling

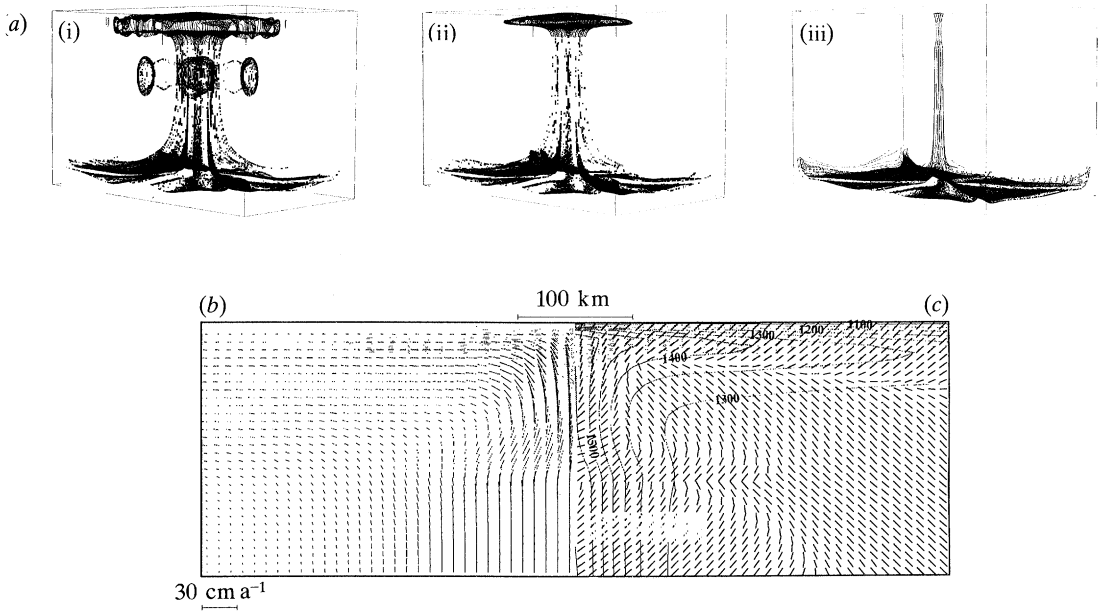

Figure 1. (*a*) Three isothermal surfaces in the area of ascending flow of the convective model: (i) 1290 °C, (ii) 1350 °C, (iii) 1500 °C. (*b*) Solidus (pale shading), cpx-out (intermediate shading) and opx-out (dark shading) boundaries according to Takahashi (1986) and Herzberg *et al.* (1990) for the upper third of the convective box in the area of ascending flow. The velocity field is shown on the left and the maximum compressive stress orientation is shown on the right.

currents, their stability through time spans of the order of hundreds of millions of years, their robustness relative to destabilizing influences like the drift of overlying plates, and their topographic and gravimetric signature.

The purpose of the present study is to compare a convective thermal field with the petrology of hotspot lavas, and we therefore need to reach realistic conditions for upper mantle convection. Accordingly, a 3D model with a Rayleigh number

$$Ra = g\alpha\,\Delta T d^3/\kappa\nu \tag{1}$$

of 10^6 has been run. The gravity constant g is 10 m s^{-2}, the coefficient of thermal expansion α is 3.7×10^{-5} °C^{-1}, the upper mantle thickness d is 6.5×10^5 m and the thermal diffusivity κ is 8×10^{-7} m^2 s^{-1}. The kinematic viscosity μ at depths greater than 150 km is 10^{17} m^2 s^{-1} and is reduced by a factor of 50 above this interface. The Rayleigh number is calculated by reference to the high viscosity. Heating is from below with a temperature contrast ΔT of 800 °C between the bottom and the top boundaries with no slip boundary conditions. The calculation has been conducted in a box with a grid meshing of $(96\times64\times96)$ and horizontal dimensions of $(3/4)^{\frac{1}{2}}d$ and $1.5d$. This aspect ratio favours the development of hexagons with a wavenumber of $\frac{4}{3}\pi$. Details of the modelling can be found in Rabinowicz *et al.* (1990).

A 3D representation of the thermal field is given in figure 1*a*. A cross section through the upper third of the box is shown on figure 1*b*, *c*. Scaling of the potential temperature has been done by assuming a value of 1280 °C in the core of the cell, according to McKenzie & Bickle (1988). This choice leads to a temperature of 1070 °C at the top of the box, compatible with the base of the lithosphere, and of 1870 °C at the upper–lower mantle transition zone, which falls in the range of estimations for the spinel–perovskite phase transition (Gasparik 1990). The heat flow transferred

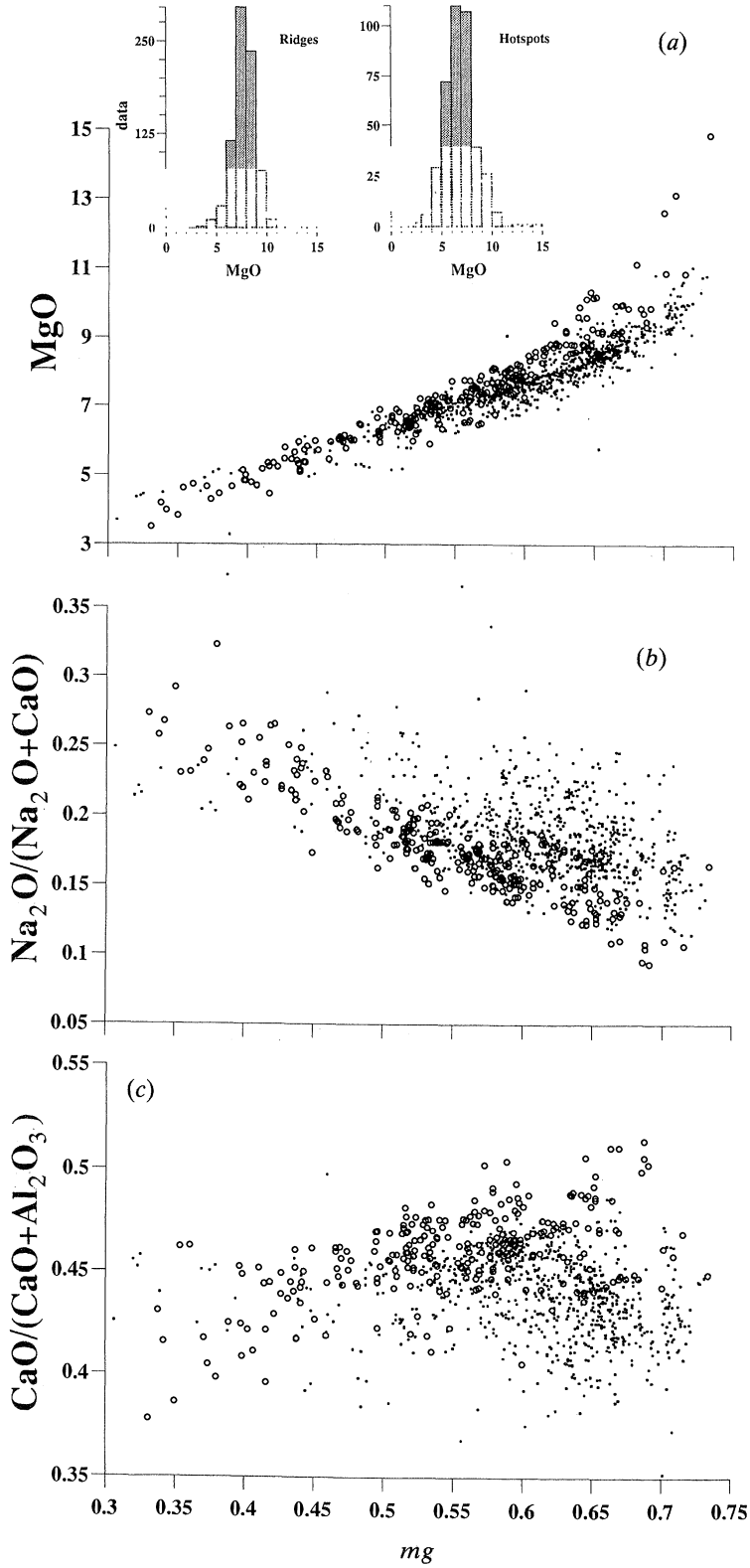

PHILOSOPHICAL TRANSACTIONS OF THE ROYAL SOCIETY A MATHEMATICAL, PHYSICAL & ENGINEERING SCIENCES

to the surface by the circulation is 60 mW m^{-2}. The plume is characterized by a relatively broad zone of gentle horizontal temperature gradient, surrounding a narrow central pipe with very steep gradients where the temperature rises by about 200 °C on a horizontal distance of a few tens of kilometres. The most striking characteristic of this thermal field is that a high temperature contrast (250–300 °C) between the core of the plume and the surrounding mantle is maintained up to the base of the upper thermal boundary layer. The flow velocity in the high viscosity layer is of the order of 70 mm a^{-1} in the plume and of 10 mm a^{-1} in the downwelling currents (not shown). This asymmetry reflects the hexagonal planform of the circulation. When it crosses the viscosity discontinuity, the ascending flow is focused towards the plume axis and the velocity increases up to 400 mm a^{-1} (figure 1*b*). Inside the LVZ, most of the plume material (about 75%) is channelled in a pipe 100 km in diameter, corresponding roughly to the thermal conduit, and will experience a large amount of adiabatic decompression due to the thinness of the upper convective boundary layer.

3. Partial melting within the plume: comparison with the composition of hotspot lavas

The solidus envelope for dry peridotite, determined experimentally by Takahashi (1986, 1990) and Herzberg *et al.* (1990), is shown on figure 1*b*, assuming an overlying lithosphere thickness of 20 km, which represents a situation of an on ridge hotspot like Iceland. Melting initiates at a depth of about 150 km, i.e. close to the base of the LVZ. Assuming no extraction, the melt fraction can easily be computed from this thermal structure. However, the melt fraction as a function of P, T is still not well determined at high pressure. We prefer to consider the composition of the residue of melting for which there are more reliable experimental constraints. The cpx-out and opx-out boundaries according to Takahashi (1986) are reported in figure 1*b*, *c*. In an area about 100 km in width at the top of the plume, the residue of melting should be dunitic, which corresponds to the production of highly magnesian melts ([MgO] > 25%). About 75% of the plume material is channelled into this shallow high temperature region, and most of the melt erupted at hotspots is likely to be extracted from the zone, at the base of the lithosphere, where high flow rates are realized and where the vertical flow rotates abruptly to the horizontal (Watson & McKenzie 1991). Massive eruptions of picritic melts should therefore be observed at hotspot volcanoes. It can of course be argued that the melt will separate from the plume as soon as the melt fraction exceeds several percent. Accordingly, the melts erupted at hotspots should result from lower degrees melting, but at high pressure. As the solidus composition at pressures around 5 GPa is komatiitic (Herzberg *et al.* 1990), this scenario also predicts the eruption of highly magnesian lavas.

To compare the predictions of the plume model with melt compositions observed at hotspot volcanoes, we have compiled about 1200 published analyses of glasses or, when not available, of aphyric lavas (phenocrysts content less than 1%). These analyses come from the worldwide oceanic ridges system and from several hotspots, mostly Hawaii and Iceland, where large volumes of tholeiitic basalts are erupted.

Figure 2. Variation diagrams for mid-ocean ridge basalts (dots) and hotspot (mainly Hawaii and Iceland) tholeiites (open circles). Only glasses and aphyric lavas are included in the data base (references available on request).

PHILOSOPHICAL TRANSACTIONS OF THE ROYAL SOCIETY A MATHEMATICAL, PHYSICAL & ENGINEERING SCIENCES

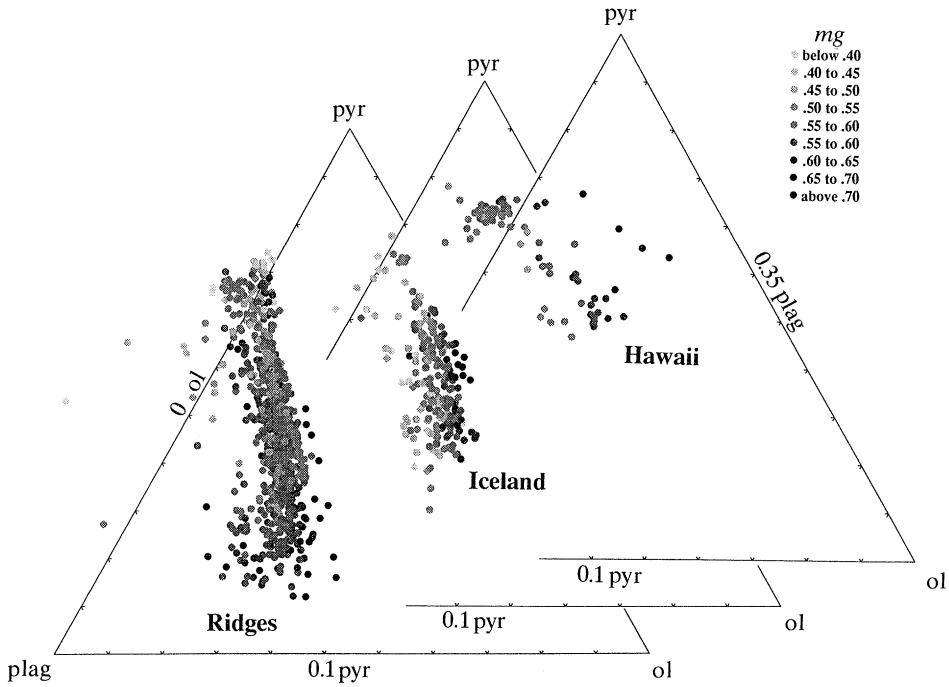

Figure 3. Plot of the same data in triangular diagrams following the projection of Bryan & Dick (1982); ol, normative olivine; pyr, normative clino- + ortho- pyroxene; plag, normative plagioclase.

The diagrams presented in figures 2 and 3 are just devoted to illustrate some basic similarities and differences between MORBs and hotspot tholeiites that any model should reproduce. Only trends of general application are presented here for the sake of discussion. An exhaustive analysis of major element chemistry of basalts can be found in Langmuir *et al.* (1992) and in Albarède (1992).

Figure 2*a* shows that the range of MgO contents of MORBs and of hotspot lavas (melts) overlap. In both environments, the average MgO content is of the order of 7 %. Maximum MgO contents for ridges and hotspots are 11 % and 15 % respectively, but it has to be stressed that MgO contents of more than 11 % are very uncommon (Clague *et al.* 1991). On figure 3, it appears that the shallow differentiation trends for ridges, Iceland and Hawaii are increasingly dominated by olivine crystallization, a characteristic which supports the view that the Hawaiian parental melt is significantly more mafic than that of MORBs, and that the one of Iceland is intermediate. However, high degree of melting followed by huge amount of low pressure fractionation cannot be invoked to explain the MgO content of hotspot tholeiites similar to those of MORBs, because the range of *mg* is similar in both environments (figure 2*a*). The slight Fe enrichment of hotspot tholeiites compared to MORBs (lower *mg* for the same MgO content, figure 2*a*) can be attributed to slightly higher amount of fractionation, but also to higher pressure of melting or to source heterogeneity (Klein & Langmuir 1987; Albarède 1992). High amount of olivine fractionation is also in contradiction with minor and trace element data (Budhan & Schmitt 1985; Feigenson 1986). Picritic lavas are observed at hotspot volcanoes, although in small amount compared to tholeiites (Nicholls & Stout 1988). However, these lavas are, as a rule, highly olivine phyric and their high MgO content reflects likely some olivine accumulation process. Such picrites are also sampled along mid-

oceanic ridges far from any hotspot. Their occurrence cannot be used as an evidence for very high degrees of melting at hotspots.

For a given *mg*, the Na/Ca ratio is sensitive to the degree of shallow melting (Allan *et al.* 1987), although this character could be attributed to source heterogeneity (Albarède 1992). Figure 2*b* shows that hotspot and ridge data have overlapping variation fields for this character also and define similar trends, in spite of a higher scatter toward high Na/Ca values (low degrees of melting) is observed for ridges.

The most primitive (high *mg*) hotspot tholeiites have significantly higher Ca/Al ratio than MORBs (figure 2*c*). This difference results in a shallow differentiation trend which appears more dominated by olivine and clinopyroxene fractionation (positive slope) at hotspots than at ridges, where the trend is rather controlled by olivine and plagioclase fractionation (negative slope). This is one example among others of geochemical trends which differ in hotspot and ridge environments.

According to this brief overview, melts produced at hotspots have a composition which has been buffered in a field similar to that of MORBs when they reach the surface. No evidence of very high degree of melting, as predicted by plume models, can be found in melts erupted at hotspot volcanoes. However, in spite of these common character, significant differences appear in the differentiation trends of hotspot and ridge tholeiites and in trace elements patterns (not shown here) which indicate that different processes are involved in the genesis of the two suites. As shown by Langmuir *et al.* (1992) and Albarède (1992), these contrasting trends cannot be explained by shallow (intracrustal) differentiation alone but require differences in the high-pressure processes. In the next section, we propose a possible scenario which might account for some of these data.

4. Discussion: consequence of melt migration within the melting region of the plume

The lack of high MgO liquids at hotspot volcanoes can be accounted for in various ways. For example, Watson & McKenzie (1991) show, in the frame of a constant mantle viscosity convective model, that the melt composition averaged on the entire melting region of the plume can fit the parental melt composition assumed for Hawaiian tholeiites by adjusting the thickness of the overlying lithosphere. This model is attractive as the lithospheric thickness they found (about 70 km) is compatible with geophysical observations at Hawaii. However, it does not account for the lack of systematic variation in melt composition with lithospheric thickness from one hotspot to the next which suggests that processes independent of the amount of adiabatic decompression control the melt composition. A thick lithospheric lid obviously cannot be invoked at on-ridge hotspots.

Another plausible explanation has been proposed by Stolper & Walker (1980) who suggest that the lack of picritic liquids at the surface is just a consequence of their high density. In that frame, low pressure crystallization of olivine, clinopyroxene and plagioclase at a pseudo-eutectic point might account for the homogeneity of eruption temperatures. However, it seems that such a 'petrological buffering' cannot be invoked in the case of the most primitive melts erupted at ridges and hotspots, as they were crystallizing one or two phases only at the time they were frozen. It means that the low temperature region of the phase diagram was never reached by these melts. For instance, clinopyroxene is observed to join olivine and plagioclase as a phenocryst in the case of highly evolved MORBs only ($0.45 < mg < 0.60$) (Hess 1989).

The wide scatter of data in variation diagrams of figures 2 and 3 is a further evidence that an invariant point was reached neither by MORBs nor by OIBs.

Here, we propose an explanation to the low eruption temperature of hotspot lavas based on the possible behaviour of the first melt fractions produced in a mantle plume. Observations in mantle outcrops show that melt migration does not involve homogeneous intergranular porous flow on distances exceeding a few metres; compaction of a crystal mush (the likely physical state of a partially molten peridotite when it crosses its solidus) induces strong lateral porosity variations and causes the redistribution of the melt in a vein network whose preferred orientation is conditioned by the local stress field (Ceuleneer & Rabinowicz 1992). Classical vein thickness (E), spacing (f) are respectively 10–100 mm and 1–100 m. The size of the veined region is typically 1–10 km. This observation is corroborated by the theoretical model of Stevenson (1989) which show that in the partly molten mantle, where the compaction length (l) is estimated to several hundred metres, the melt is distributed in regions of high melt/rock ratio (veins) oriented parallel to the maximum compressive stress (σ_1) whose spacing (f) is proportional to $(lr)^{-\frac{1}{2}}$ where r is the grain radius of mantle rocks, i.e. f is of the order of 1 m. Although they are preferentially oriented along the σ_1 direction, the close spacing of the veins compared to their length implies connectivity of the veins. Furthermore, connection of the veins will eventually lead to their coalescence and will trigger the development of extremely long veins (Sleep 1988). It results that a network of veins oriented along the σ_1 direction and extending across the whole partially molten region will develop. The effective permeability K of this system along the σ_1 direction is given by the Hele–Shaw relation:

$$K = E^3/12\,f. \tag{2}$$

In the case of 5% melt fraction distributed in veins with $f = 1$ m, the permeability K is about 10^{-5} m^2.

From the base of the melting region to depths of around 80–100 km, σ_1 is sub-horizontal; its dip is of the order of 10–20° toward the axis of the plume (figure 1*b*). The extension direction (not shown) is sub-vertical. Accordingly, a network of sub-horizontal veins radiating away from the plume axis will develop in this lower part of the melting region. Assuming this system is interconnected, buoyancy forces could lead to initiation of hydrofracturing which would result in rapid melt migration to the surface (Nicolas 1986). However, due to the small density contrast between melt and solid at such pressures (Herzberg 1987), and to the sub-horizontal attitude of the veins, hydrofracturing can only occur if interconnection extends for a few hundred kilometres at least which exceeds the dimension of the melting region! The melt will thus remain trapped within the vein network. The conclusion that hydrofracture is unlikely even in the shallow asthenosphere is corroborated by observations in ophiolites which show that dyking is absent from zones of palaeovertical mantle flow and is typically an off-axis mechanism. Melt percolation in a network of close spaced veins is found to be the dominant migration mechanism in mantle diapirs (Ceuleneer & Rabinowicz 1992).

If hydrofracture does not occur, the strong temperature contrast between the centre and the periphery of the plume will probably induce convection of the melt within the vein network. Due to the geometry of the system, flow can be described as Hele–Shaw convection in an inclined layer. The porous Ra number is:

$$Ra_{\mathrm{p}} = \alpha_1 \Delta T g \sin(\Theta) LK/\kappa\nu_1, \tag{3}$$

where α_l and ν_l are the coefficient of thermal expansion and the viscosity of the liquid, Θ the dip of σ_1, L is the interconnection length along the σ_1 direction and ΔT is the temperature contrast between the centre and the periphery of the melting region. For high pressure melts, α_l is of the order of $10^{-4}\,°C^{-1}$ and ν_l of the order of $10^{-3}\,m^2\,s^{-1}$ (Kushiro 1980; Herzberg 1987).

Figure 1*b*, shows that L may reach a value of about 50 km at depths around 100 km, if interconnection is achieved from the centre to the periphery of the melting region; Θ is of the order of 20° and the thermal contrast is of the order of 150 °C. This lead to an estimation for Ra_p of the order of 2.5×10^7. This is a huge value for porous flow convection, and shows that a large amount of heat can be advected by melt circulation. The effective diffusivity of heat within the melting region can be estimated using

$$\kappa_{ef} = \kappa Nu, \tag{4}$$

where Nu is the Nusselt number of the porous flow convection. Recent estimations of the relation $Nu\,f(Ra)$ for large values of Ra give (Lister 1990):

$$Nu = 0.45\,Ra^{0.55}. \tag{5}$$

Accordingly, values for Nu greater than 10^3 are possible, and will promote the rapid homogenization of the plume temperature. A characteristic time of attenuation of the thermal contrast existing in a finite circular tube is given by (see Carslaw & Jaeger 1978, p. 195):

$$a^2/\kappa_{ef}\,\beta^2, \tag{6}$$

where $\beta = 2.4048$, is the smallest root of the Bessel function of order 0. According to the above estimates, temperature homogenization could be achieved in less than 2×10^4 years, the time needed by the mantle plume to rise by about 10 km. This reasoning shows that complete homogenization of the plume temperature can be achieved due to porous flow convection in the vein network as soon as the melting region has reached a sufficiently large horizontal extension. We have calculated that if the temperature is fully homogenized in the thermal conduit, conservation of the heat advected by the plume requires a plume temperature exceeding the temperature of the surrounding mantle by about 50 °C.

According to observations in mantle outcrops, interconnection is achieved as soon as the melt fraction exceeds several percent which will occur at high pressure when the temperature exceeds the solidus temperature by a small amount (Takahashi 1986; Herzberg *et al.* 1990). Higher degree of melting will not be realized as the heat released by further decompression will be removed from the high temperature region of the plume by melt convection. Melt will also undergo fractional crystallization as it moves toward the periphery of the plume, which will progressively increase its fluid and LIL contents. Starting with a komatiitic liquid, the solidus composition at 5 GPa (Herzberg 1990), the melt will evolve mainly in response to crystallization of olivine and garnet: a Ca-poor garnet has been shown to follow olivine in the crystallization sequence of a komatiite around 5 GPa, while pyroxene joins these two phases later on (Herzberg *et al.* 1990). Garnet crystallization will induce some characteristic trends in both major and trace element compositions of the residual liquid, like a high Ca/Al and a high La/Yb. It is tentatively proposed that, in the lower part of the melting region (5–3 GPa), the melt circulating in the drainage network acquires progressively a kimberlitic composition, which is intermediate between an ultrabasic and an alkalic end member and displays some of the geochemical characters

PHILOSOPHICAL TRANSACTIONS OF THE ROYAL SOCIETY A MATHEMATICAL, PHYSICAL & ENGINEERING SCIENCES

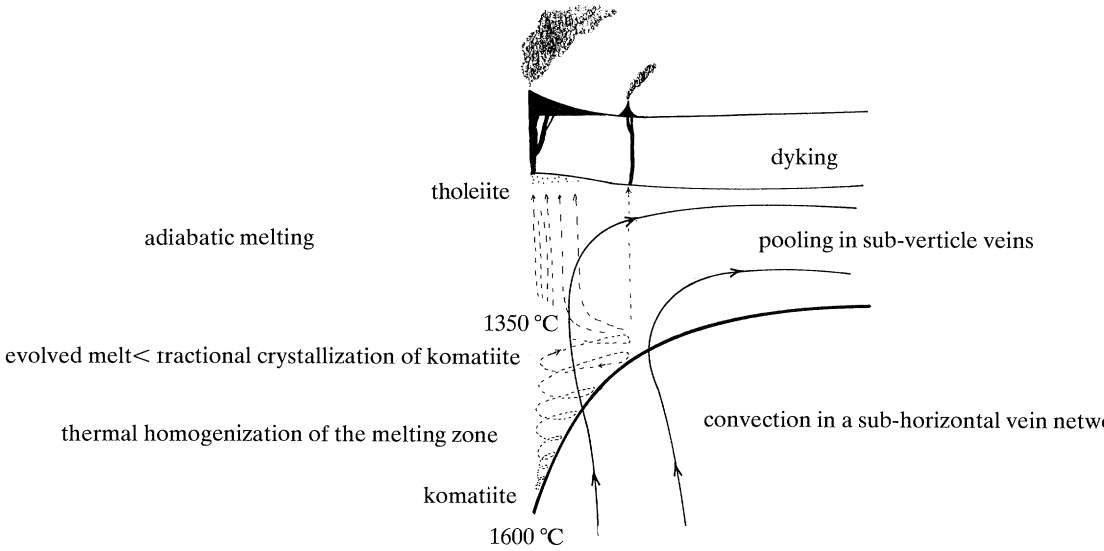

Figure 4. Sketch illustrating solid-state flow trajectories (solid lines) and melt flow trajectories (dashed lines) in the melting region of the convective plume. The heavy curve is the solidus.

mentioned above (Wyllie 1988). The progressive increase of the fluid content can promote remelting of the wall rock by lowering its solidus temperature (Wyllie 1988), and will prevent complete 'freezing' of the melt drainage system. Here again, a kimberlitic melt will be produced as shown by high pressure melting experiments in conditions of CO_2 saturation (Canil & Scarfe 1990). In the case of a very thick lithospheric lid (craton) overlying the plume, this melt may reach the surface. In the case of a thinner lithosphere, the composition of the melt circulating in the vein network will continue to evolve in response to both fractional crystallization and introduction of lower pressure melt fractions at the periphery of the plume (figure 4). Among other effects, these two processes will contribute to lower the Mg content of the melt and may move its composition toward the one of an alkalic lava. Finally, where there is no obstacle to further decompression (on-ridge hotspot or deeply eroded lithosphere), a large volume of the plume will melt as the solidus envelope enlarges (figure 4). However, the temperature in the melting region is buffered to a value close to the average mantle potential temperature, and the plume will produce a tholeiitic melt. Since the maximum compressive stress is now sub-vertical, melt fractions will collect in steeply dipping veins and eventually cracks which will trigger rapid melt migration toward the surface. The lavas erupted at hotspots are likely to result from the mixing in various proportion of these tholeiites with the residual melts produced in the lower part of the melting zone. This process may account for some petrological peculiarities (relative to MORBs of similar *mg*) of hotspot tholeiites, like their 'enriched' signature and other geochemical characters discussed above.

There are two assumptions which are critical for the present model: (i) partial melting of the plume is associated with a viscosity drop which induces the focusing of the mantle flow and, consequently, a sub-horizontal orientation of the maximum compressive stress; (ii) that intergranular partial melt is not stable in intergranular position but migrates to form a vein network. These two points are among the most firmly established conclusions derived from structural observations in mantle outcrops. There is of course no direct evidence that the interplay between solid-state

flow and melt migration follows the same modalities at 150 km depth. However, if both assumptions are valid, they imply that melt differentiation and thermal homogenization will take place in the melting region of mantle plumes.

This work has greatly benefited from discussions with Peter Kelemen and Claude Dupuy, and from a constructive review of Dan McKenzie. We are very indebted to Philippe Vidal for his repeated encouragements to pursue this direction of research. This is a contribution CNRS–INSU, programme DBT, thème 'Instabilités', no. 476.

References

Albarède, F. 1992 How deep do common basaltic magmas form and differentiate ? *J. geophys. Res.* **27**, 10997–11009.

Allan, J. F., Batiza, R. & Lonsdale, P. 1987 Petrology of lavas from seamount flanking the East Pacific Rise axis at 21° N: implications concerning the mantle source composition for both seamount and adjacent EPR lavas. In *Seamounts, islands and atolls*, pp. 255–282. AGU Monographs.

Bryan, W. B. & Dick, H. J. B. 1982 Contrasted abyssal basalt liquidus trends: evidence for mantle major element heterogeneity. *Earth planet. Sci. Lett.* **58**, 15–26.

Budhan, J. R. & Schmitt, R. A. 1985 Petrogenetic modeling of Hawaiian tholeiitic basalts: a geochemical approach. *Geochem. cosmochim. Acta* **49**, 67–87.

Canil, D. & Scarfe, C. 1990 Phase relations in peridotites + CO_2 systems to 12 Pa: implications for the origine of kimberlite and carbonate stability in the Earth's upper mantle. *J. geophys. Res.* **95**, 15805–15816.

Ceuleneer, G. & Rabinowicz, M. 1992 *Mantle flow and melt migration beneath oceanic ridges: models derived from observations in ophiolites* (ed. D. Blackman & J. Phipps Morgan). AGU Monographs. (In the press.)

Ceuleneer, G., Rabinowicz, M., Monnereau, M., Cazenave, A. & Rosemberg, C. 1988 Viscosity and thickness of the sublithospheric low-viscosity zone: constraints from geoid and depth over oceanic swells. *Earth planet. Sci. Lett.* **89**, 84–102.

Clague, D. A., Weber, W. S. & Dixon, J. E. 1991 Picritic glasses from Hawaii. *Nature, Lond.* **353**, 553–556.

Feigenson, M. D. 1986 Constraints on the origin of Hawaiian lavas. *J. geophys. Res.* **91**, 9383–9393.

Gasparik, T. 1990 Phase relations in the transition zone. *J. geophys. Res.* **95**, 15751–15769.

Helz, R. T. 1987 Diverse olivine types in lava of the 1950 eruption of Kilauea volcano and their bearing on eruption dynamics. *U.S. Geol. Survey. Prof. Papers* **1350**, 691–722.

Herzberg, C. T. 1987 Magma density at high pressure. Part 1. The effect of composition on the elastic properties of silicate liquids. *Geochem. Soc. Spec. Publ.* **1**, 25–46.

Herzberg, C., Gasparik, T. & Sawamoto, H. 1990 Origin of mantle peridotite: constraints from melting experiments to 16.5 GPa. *J. geophys. Res.* **95**, 15779–15804.

Hess, P. C. 1989 *Origins of igneous rocks.* (336 pages.) Harvard University Press.

Jakobsson, S. P., Jonsson, J. & Shido, F. 1978 Petrology of the western Reykjanes peninsula, Iceland. *J. Petrol.* **19**, 669–705.

Klein, E. M. & Langmuir, C. H. 1987 Global correlations of ocean ridge basalt chemistry with axial depth and crustal thickness. *J. geophys. Res.* **92**, 8089–8115.

Kushiro, I. 1980 Viscosity, density, and structure of silicate melts at high pressure, and their petrological applications. In *Physics of magmatic processes* (ed. R. B. Hargraves), pp. 93–120. Princeton University Press.

Langmuir, C., Klein, E. & Plank, T. 1992 *Petrological constraints on melt formation and segregation beneath MOR* (ed. D. Blackman & J. Phipps-Morgan). AGU Monograph. (In the press.)

Lister, C. R. B. 1990 An explanation for the multivalued heat transport found experimentally for convection in a porous medium. *J. Fluid Mech.* **214**, 287–320.

McKenzie, D. P. & Bickle, M. J. 1988 The volume and composition of melt generated by extension of the lithosphere. *J. Petrol.* **29**, 625–679.

Nicolas, A. 1986 Melt extraction model based on structural studies in mantle peridotites. *J. Petrol.* **27**, 999–1022.

Nicholls, J. & Stout, M. Z. 1988 Picritic melts in Kilauea – evidence from the 1967–1968 Halemaumau and Hiiaka eruptions. *J. Petrol.* **29**, 1031–1057.

Rabinowicz, M., Ceuleneer, G., Monnereau, M. & Rosemberg, C. 1990 Three-dimensional models of mantle flow across a low viscosity zone: implications for hotspot dynamics. *Earth planet. Sci. Lett.* **99**, 170–184.

Robinson, E. M., Parsons, B. & Daly, S. F. 1987 The effect of a shallow low viscosity zone on the apparent compensation of mid-plate swells. *Earth planet. Sci. Lett.* **82**, 335–348.

Sleep, N. H. 1988 Tapping of melt by vein and dykes. *J. geophys. Res.* **93**, 10255–10272.

Stevenson, D. J. 1989 Spontaneous small-scale melt segregation in partial melts undergoing deformation. *Geophys. Res. Lett.* **16**, 1067–1070.

Stolper, E. M. & Walker, D. 1980 Melt density and the average composition of basalt. *Contrib. Mineral. Petrol.* **74**, 7–12.

Takahashi, E. 1986 Melting of a dry peridotite KLB-1 up to 14 GPa: implications on the origin of peridotitic upper mantle. *J. geophys. Res.* **91**, 9367–9382.

Watson, S. & McKenzie, D. P. 1991 Melt generation by plumes: a study of Hawaiian volcanism. *J. Petrol.* **32**, 501–537.

White, R. S. & McKenzie, D. P. 1989 Magmatism at rift zones: the generation of volcanic continental margins and flood basalts. *J. geophys. Res.* **94**, 7685–7729.

Wyllie, P. J. 1988 Magma genesis, plate tectonics and chemical differentiation of the Earth. *Rev. Geophys.* **26**, 370–404.

PHILOSOPHICAL TRANSACTIONS OF THE ROYAL SOCIETY A MATHEMATICAL, PHYSICAL & ENGINEERING SCIENCES

Figure 1. (*a*) Three isothermal surfaces in the area of ascending flow of the convective model: (i) 1290 °C, (ii) 1350 °C, (iii) 1500 °C. (*b*) Solidus (pale shading), cpx-out (intermediate shading) and opx-out (dark shading) boundaries according to Takahashi (1986) and Herzberg *et al.* (1990) for the upper third of the convective box in the area of ascending flow. The velocity field is shown on the left and the maximum compressive stress orientation is shown on the right.